Electronic Supplementary Material (ESI) for RSC Advances.

Synthesis of a low-density biopolymeric chitosan-agarose cryomatrix and its surface functionalization with bio-transformed melanin for the enhanced recovery of uranium (VI) from the aqueous sub-surfaces

Anuj Tripathi and Jose Savio Melo*

Nuclear Agriculture and Biotechnology Division, Bhabha Atomic Research Centre, Mumbai-400085, India

Supplementary Information

1. Methodology

1.1. Morphology and porosity analysis

AC and MAC cryomatrices were morphologically examined for determining the size and distribution of pores in respective matrices using scanning electron microscope (SEM). Porosity of these cryomatrices was calculated theoretically according to the Archimede's principle and using the equation 1;

$$\text{Porosity} = (M_W - M_D)/ (M_W - M_{SUB}) \quad (1)$$

where, M_W is the water saturated wet mass of the scaffold, M_D is the dry mass of the scaffold, and M_{SUB} is the submerged mass of the scaffold.

1.2. Swelling kinetics and swelling ratio

The swelling behavior of AC and MAC cryomatrices was examined at different time intervals in dH_2O at 27 ± 1 °C till the matrix reached its swelling equilibrium. The swelling kinetics (S_K) and swelling ratio (S_R) were calculated using the equations 2 & 3;

$$S_K = [(W_T - W_D)/ W_E] \times 100 \quad (2)$$

$$S_R = (W_E - W_D) / W_D \quad (3)$$

where, S_K is the swelling kinetics and S_R is swelling ratio of the matrix, W_D is the dry weight of the matrix, W_E is the wet weight of the matrix at swelling equilibrium and W_T is the wet weight of the matrix at different time intervals.

1.3. Hydraulic permeability analysis

The relationship between the flows of liquid through porous matrix with a constant hydraulic pressure defines the hydraulic permeability of that matrix, which was determined using Darcy's law.[11,S1] The AC and MAC matrices (8 mm diameter, 5 mm height) were placed in the permeability measurement setup and under a constant water pressure head, flushed water was collected for 2 min from the outlet. As a control, no matrix was placed between the flow-path. The hydraulic permeability was calculated using the equation 4;

$$\kappa = \frac{\Delta X}{A \times M_{B2}} \times \frac{2\pi^2 r^4}{\left(M_{B1}/M_{B2}\right)^2 - 1} \quad (4)$$

where, κ is the hydraulic permeability of the matrix, A is the flushing area of the matrix, ΔX is the thickness of matrix, M_{B1} and M_{B2} are the mass of water flushed from the outlet in control and test, respectively.

1.4. Density analysis

The density (ρ) of cryomatrices (g cm^{-3}) was calculated using their respective mass (M) and volume ($4/3\pi\ r^3$) either in wet or dry condition from equation 5;

$$\rho = M / [4/3\pi\ r^3] \quad (5)$$

1.5. *In-vitro* degradation analysis

In-vitro degradation of AC and MAC cryomatrices was carried out by incubating in dH_2O at 37 °C ± 1 for four weeks under non-stirring condition. Three samples were taken out every week and washed with dH_2O followed by drying at 60 °C. The dry weights of degraded samples were recorded for calculating the degree of degradation using the equation 6;

$$D_D\ (\%) = 100 \times (W_I - W_F)/W_I \quad (6)$$

Where, D_D is degree of degradation, W_I is initial dry weight and W_F is final dry weight of cryomatrix.

1.6. Zeta potential analysis

Zeta potential of AC and MAC cryomatrices was determined at different pH. Processing of solid samples was performed for zeta potential analysis as per the previously reported study.[11] Briefly, cryomatrices were dried (~20 mg dried mass) at 60 °C for 4 h followed by grinding of matrices using mortar and pestle. A fine powder of respective matrices was obtained, which was further sieved using membrane filter (perture size: 53 µm; BSS-300, Jayant Scientific Industries, Mumbai, India). The particles (≤ 53 µm) of cryomatrix were suspended in 10 mL of dH_2O. The suspension was dispensed into different vials and pre-assigned pH values (pH 3 to 11) were adjusted using 1 N HCL and 1 N NaOH solutions without addition of background electrolytes. The suspensions of different pH were then incubated at 27 ± 1 °C for 24 h and further analyzed using a Zetasizer analyzer (Nano-Z series, Malvern, UK).

1.7. Thermo gravimetric analysis

Thermo-gravimetric analysis (TGA) (NETZSCH Thermal analyzer; STA 409 pc Luxx, GMBH) of AC and MAC cryomatrices was conducted from 30 to 700 °C with a heating increment of 10 °C min^{-1} in an inert atmosphere. The obtained values were used for the interpretation of thermal properties of both the cryomatrices.

1.8. Fourier transform infrared spectroscopy

The fourier transform infrared (FT-IR) spectroscopy of AC and MAC cryomatrices was performed using FT/IR-660 Plus spectrophotometer (Jasco, Japan) and analysed for

understanding the chemical attribution in the matrices and also for the confirmation of the binding of uranyl ions.

1.9. Rheological characterization

The rheological characterization of AC, MAC and after uranium sorption i.e. MAC-U was performed on Rheometer-MCR 102 (Anton-Paar, Germany) at 27 ± 1 °C. Matrix as a single bead form was placed between the measuring plates and a gradually increasing force was applied from 1 N to 50 N at a fixed frequency (1Hz) and amplitude (0.1%). The associated software RHEOPLUS was used to record the different variables such as elastic modulus (G') and loss modulus (G"), which were further used to calculate the complex modulus (G*) of the cryomatrices.

1.10. Quantification of uranium

Quantification of uranium present in the solution before and after sorption and desorption experiment was spectrophotometrically quantified using Arsenazo (III) method. 0.1 mL of 0.05% Arsenazo (III) (HiMedia, India) solution prepared in dH_2O was added to 0.1 mL of 4% aqueous oxalic acid. 0.5 mL test sample was mixed to this solution followed by addition of 2.5 mL HCl (4 M), which was examined spectrophotometrically at 650 nm. The minimum sensitivity of the method is 1 mg L^{-1}.

1.11. Statistical analysis

For the statistical analysis, samples were studied in triplicate for all the experiments. The obtained experimental values are presented as mean ± standard deviation (SD) and the data analysis was performed with one-way ANOVA using *Tukey's* honestly significant difference (*Tukey HSD*) test in SPSS software (version 10) and differences were considered significant at $P < 0.05$.

2. Results and discussion

2.1. Drawbacks of classical hydrogels

Use of polymeric biomaterials in their native form has several limitations like poor mechanical strength which leads to difficulty in handling, presence of multi-functional moieties, low resistance to degradation and poor recovery after application. Casting these polymers in hydrogel form is also associated with disadvantages like poor mass transport ability and slow rate of swelling due to the presence of very small pores.[S2] Insufficient mechanical stability also does not persuade the appropriate utilization of such biopolymeric materials.[S3] Another drawback is the designing of biopolymer matrix in different formats by classical approaches which imparts inherent high density to the gels resulting in the sinking of gels in aqueous system. These properties of classical adsorbents are inappropriate for the uranium recovery from the aqueous sub-surfaces.

2.2. Effect of cryo-polymerization

The aqueous polymeric drops of agaorse-chitosan adopt the spherical shape in the moderately frozen paraffin oil medium at the sub-zero temperature (−20 °C). Continuous incubation of these polymeric beads at sub-zero temperature leads to phase seperation, where the aqueous phase get separated from the polymeric phase and form ice-crystals that act as a porogen. On the other hand, the unfrozen polymeric phase get crosslinked in the presence of glutaradehyde and form a water insoluble polymeric network. After completion of incubation at −20 °C for 16 h, these matrices were seived from parafin oil and thawed in dH_2O. The ice crystals disappear during thawing at room temperature leaving a void space, result in a porous 3D archetecture was obtained.

2.3. Optimization of $_L$-DOPA concentration

In general, melanin is balckish-brown in color when obtained by sequestrial oxidative conversion of $_{L}$-DOPA.[10] Priliminary experiment suggested that low molar concentration of $_{L}$-DOPA is more suitable to control the size of melanin molecules. This is in agreement with the limited availability of precusor molecules for biogenic transformation, followed by interaction of identical entity to form a bigger molecule. High concentration of $_{L}$-DOPA (30 mM) allowed the formation of large polymerized particles of melanin in the solution. Thus the lower concentrations (i.e. 1, 5, 10 and 20 mM) were used to optimize the surface functionalization of AC cryomatrix (data not shown). For 100 mg AC cryomatrix, the optimum concentration of $_{L}$-DOPA was 10 mM in 20 mL solution. Below this concentration, the cryomatrices were not completely saturated with blackish-brown melanin and also the rate of reaction was found to be slow. However, at higher concentrations, the melanin remained unbound to the matrix and was present in the solution.

2.4. Effect of melanin on cryomatrix morphology

The result suggest that the process of melanin functionalization did not cause significant change in the microstructure of cryomatrix and present the suitability of these cryomatrix for high flow of liquid through their pores (Table 1). The hydropylicity of melanin could be governed by the arrangement of melanin molecules with orientation of carboxylic and hydroxyl moieties. It is speculated that melanin functionalization on AC cryomatrix was an in-situ interpenetrating polymerization, which did not affect overall structural morphology of cryomatrix.

2.5. Degradation of matrix

In a control experiment, AC cryomatrix without glutaraldehyde crosslinking disapeared completely in the third week of incubation. Unlike ionic gelation (in case of control), the covalent crosslinking decreases the rate of degradation of polymer and provides better stability to

the matrix.[S4] It is presumed that the surface of polymer matrix undergoes preferential hydrolytic scission, where long polymer chains are converted into oligomeric units, which can fade out in aqueous medium.[13] In the first week, the initial weight loss in MAC cryomatrix could be because of the disintegration of loosely bound polymeric or oligomeric moieties. In consecutive weeks, the degradation was minimal and negligible weight loss was observed. However, the degradation of AC cryomatrix showed gradual increase with time as shown in Fig. 3C. The MAC cryomatrix showed increased resistance to biodegradation and suggest its potential for the recovery of heavy metal from aqueous medium. Moreover, discharge of these cryomatrices into the environment after the uranium recovery application can be considered to be a safe approach due to their non-toxic and biodegradable nature.

2.6. Surface charge analysis

The presence of electrokinetic charges on the surface can suggest a cryptic nature of a polymeric matrix and enlighten its affinity to other molecules. The electric potential between the interfacial regions near the matrix surface is defined as its zeta potential or electro-osmotic mobility. Significant variation was observed in the zeta potential (ζ) of AC and MAC cryomatrices at different pH's ranging from 3 to 11 (Fig 4B). The zeta potential of the melanin molecules at different pH was also examined to confirm its role in MAC cryomatrix. The Fig. 4B shows high net negative zeta potential of melanin in its free form, which showed steep increase in negative zeta potential from pH 3 (ζ: −15.4 ± 0.81 mV) to pH 7 (ζ: −31.8 ± 1.10 mV) and then established up to pH 11 (ζ: −33.7 ± 1.02 mV) without significant change.

2.7. Uranium sorption

Uranium sorption on polymer adsorbent could be affected by speciation of the metal ions or the ionization of functional groups on polymer depending on pH of the aqueous medium. In general,

uranyl ions exist as an aqueous mononuclear ionic form in the acidic pH, which turns into insoluble hydrolyzed oligomeric species by increasing the pH of the solution.[S5] Uranium exists in solution predominantly as UO_2^{2+}. However, between pH 4.0 and 7.5, U(VI) exists primarily in hydrolyzed forms.[38] Uranium exists in the +6 oxidation state under oxidizing to mildly reducing environments. Overall, the results indicated that the pH affected the sorption of uranium and found maximum adsorption of uranium by cryomatrix at pH 5.5, which was used in further experiments. Moreover, less amount of uranium adsorption was observed from NSW than from the ASW, which could probably due to the presence of unknown micron-size molecules that might hinder the affinity of cryomatrix to form a complex with uranyl ions.

2.8. Rheology and FTIR

Further, sorption of uranium by MAC cryomatrix was also confirmed by rheology and FTIR (results are discussed in manuscript).

In principle, polymeric materials show deformation behavior under the applied forces and provide quantitative values of material elasticity (storage modulus; G') and viscosity (loss modulus; G") under defined rheometry conditions. The relationship between G' and G" were further used to obtain the complex modulus (G*) of the cryomatrix. A study of change in G* at constant force (1N) showed no change in the G' and G" which explains that the basic property of the cryomatrix remains constant.

IR spectrum of composite AC cryomatrix represents a combination of functional groups present in the native polymer chains of agarose and chitosan. The symmetric and asymmetric stretching peaks of C−H at 2888 cm^{-1} and 2948 cm^{-1} were clearly observed in AC cryomatrix. The characteristic peaks of 3, 6-anhydro-L-galactose skeletal bending was observed at 941 cm^{-1} and 890 cm^{-1} in both AC and MAC cryomatrices, which confirms the presence of agarose. The

absorption peaks at 1072 cm^{-1} confirms the presence of saccharide structure in composite cryomatrix.[S6] Few other peaks which were found to overlap can be due to the similar functional groups in the AC and MAC cryomatrices.

2.9. Chitosan as a sorption matrix

Chitosan is available as a byproduct of marine food processing, is environmentally safe and can be a low cost adsorbent for U removal from wastewater. The naïve form of chitosan is not suitable due to its insolubility in water. Synthesis of chitosan based matrices have been achieved by dissolving it in the acidic solution and then used alone or in combination with other support matrix.[S7-S14] Also synthesis of chitosan matrix in porous form reduced its elastic property and it becomes more fragile.[11] Table S1 briefly explains various studies on chitosan and its functionalized composite along with other biosorbents for their application in uranium sorption. In contrast, the present study demonstrated the use of optimum concentration of agarose and chitosan polymer to synthesize a porous cryomatrix presenting spongy-like visco-elastic property. Further, bio-functionalization of composite agarose-chitosan cryomatrix by melanin through in-situ biocatalysis enhanced the mechanical as well as functional properties of cryomatrix. Additionally, melanin surface functionalization may also serve as a protective barrier (due to anti-microbial property) and has increased the resistance to biodegradation of biopolymeric cryomatrix compared to unmodified control matrix, which is otherwise a major drawback in biopolymer systems for their successive environmental applications. To the best of our knowledge, our group is first to introduce this novel approach of low-density polymeric cryomatrix synthesis and application in uranium recovery. In an earlier reported study, uranium recovery using alginate and agarose as precursor polymers were used to synthesize a porous matrix, which showed 120 mg g^{-1} of q_{max}. The present study demonstrates the high affinity to

uranium and more than three-fold increase U sorption capacity (q_{max}: 435 mg g^{-1}). Moreover, in comparison to the existing synthetic sorbent, MAC cryomatrix shows high uranium adsorption from the aqueous medium and its unique floating properties could be a sustainable approach for uranium recovery from aqueous sub-surfaces.

Supplementary Table

Table S1: Study of uranium recovery from aqueous medium using different biosorbents

Material	**Material state**	**Amount adsorbed (mg/g)**	**Ref.**
Human black hair	Fibrous material	62.5	4
Plant root of *E. crassipes*	Powder	371	5
Silica nanoparticles with S. lactis cells	Microparticles	169.5	6
Red algae (*C. repens*)	Whole biomass	303	8
Agarose-alginate	Porous cryomatrix	120	9
Melanin	Macroparticles	588	10
Epichlorohydrin crosslinked chitosan	Particles	52.6	S7
Chitosan-perlite	Beads	149	S8
Modified chitosan	Resins	330	S9
Chitosan	Flakes	200	S10
Chitosan	Microcrystalline	380	S11
Chitosan phosphate	Granular particles	240	S12
Chitosan coated magnetite	Nanoparticles	42	S13
Melanin-agarose-chitosan*	Porous cryomatrix	435	*Present work*

*melanin to polymer ratio is 3:20. Thus, in comparison to previous study[10], mg of uranium sorption w.r.t. per gram of melanin is much higher in the present study.

Supplementary Figures

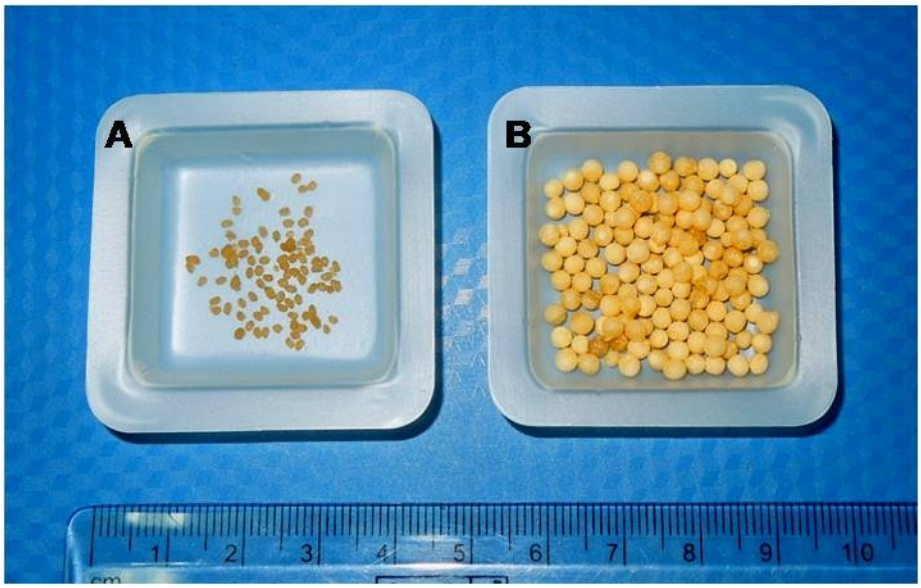

Figure S1: The dried agarose-chitosan cryomatrix in the form of beads. Image (A) shows shrinkage property of AC hydrobead when synthesized at room temperature and (B) shows the shape retaining property of cryo-polymerized AC matrix.

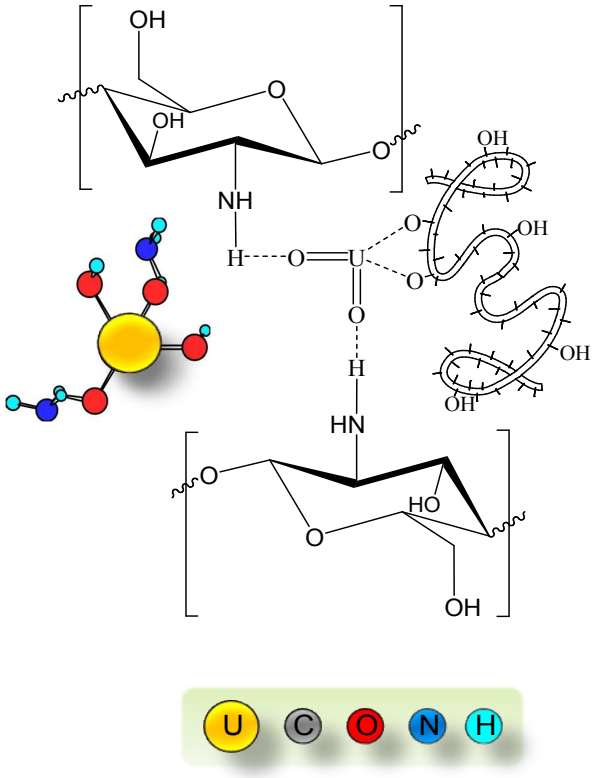

Figure S2: The possible uranyl ion interaction to the functional group of agarose-chitosan (AC) cryomatrix and its three-dimensional confirmation.

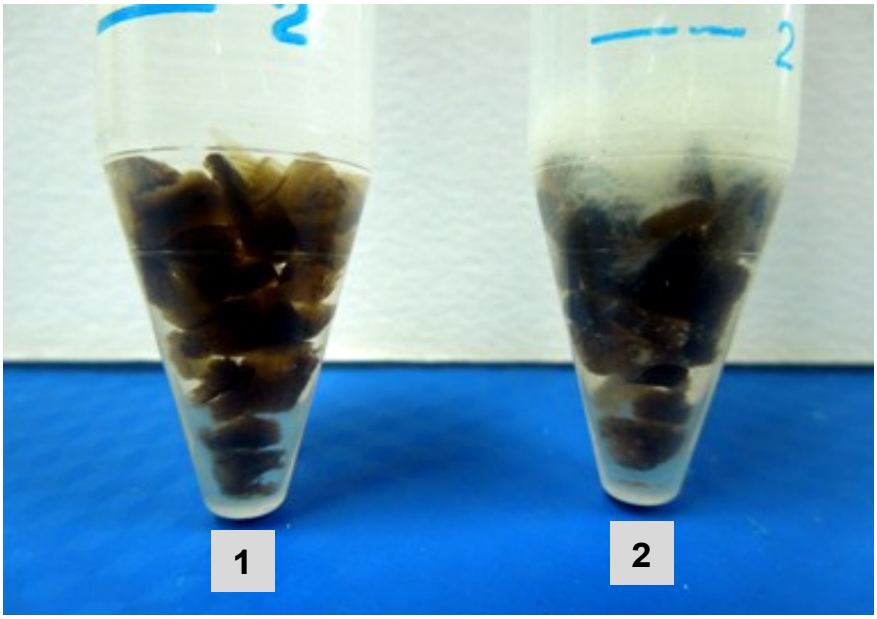

Figure S3: Image shows the long term effect of desorbent on MAC cryomatrix after incubating for 60 days at room temperature. Tube (1) contains 0.1 M HCl, and tube (2) contains 0.1 M EDTA. The MAC cryomatrix shows no effect in the color change and physical deterioration after incubating in the HCl solution, however, a prominent white color precipitate was observed in case of EDTA solution.

3. References

S1. J. Li and A.F.T. Mak, *J. Biomater. Appl.*, 2005, **19**, 253-266.

S2. E. Sachlos and J.T. Czernuszka, *Europe. Cells Mater.*, 2003, **5**, 29-40.

S3. H.T. Peng, L. Martineau and P.N. Shek, *J. Mater. Sci. Mater. Med.*, 2007, **18**, 975-986.

S4. N. Kathuria, A. Tripathi, K.K. Kar and A. Kumar, A, *Acta Biomater.*, 2009, **5**, 406– 418.

S5. C.J. Chisholm-Brause, J.M. Bergy, R.A. Matzner and D.E. Morris, *J. Colloid. Interface Sci.*, 2001, **233**, 38-49.

S6. K. Prasad, G. Mehta, R. Meena and A.K. Siddhanta, *J. Appl. Polym. Sci.*, 2006, **102** (4), 3654-3663.

S7. G. Wanga, J. Liu, X. Wang, Z. Xie and N. Deng, *J. Hazard. Mater.*, 2009, **168**, 1053–1058.

S8. S. Hasan, T.K. Ghosh, M.A. Prelas and D.S. Viswanath, *Nucl. Technol.*, 2006, **159**, 59-71.

S9. C. Gerente, Y. Andrès and P.L. Cloirec. *Environ. Technol.*, 1999, **20**, 515-521.

S10. A. Sabarudin, M. Oshima, T. Takayanagi, L. Hakim, K. Oshita, Y.H. Gao and S. Motomizu, *Anal. Chim. Acta*, 2007, **581**, 214–220.

S11. E. Piron, M. Accominotti and A. Domard, *Langmuir*, 1997, **13**, 1653-1658.

S12. E. Guibal, M. Jansson-Charrier, I. Saucedo and P.L. Cloirec, *Langmuir*, 1995, **11**, 591-598.

S13. T. Sakaguchi, T. Horikoshi and A. Nakajima, *Agric. Biol Chem.*, 1981, **45**(10), 2191-2195.

S14. L.C.B. Stopa, M. Yamaura, *Int. J. Nucl. Ener. Sci. Technol.*, 2010, **5** (4), 283–289.